Title
QUARK-GLUON PLASMA FORMATION IN THE CENTRAL RAPIDITY REGION AND FINITE SIZE EFFECTS OF COLLIDING NUCLEI

Author
Sumiyoshi, H.

Publication Date
1983-12-01

Lawrence Berkeley Laboratory
UNIVERSITY OF CALIFORNIA

Submitted to Zeitschrift für Physik

QUARK-GLUON PLASMA FORMATION IN THE CENTRAL RAPIDITY REGION AND FINITE SIZE EFFECTS OF COLLIDING NUCLEI

H. Sumiyoshi, S. Date, N. Suzuki, O. Miyamura,
and T. Ochiai

December 1983

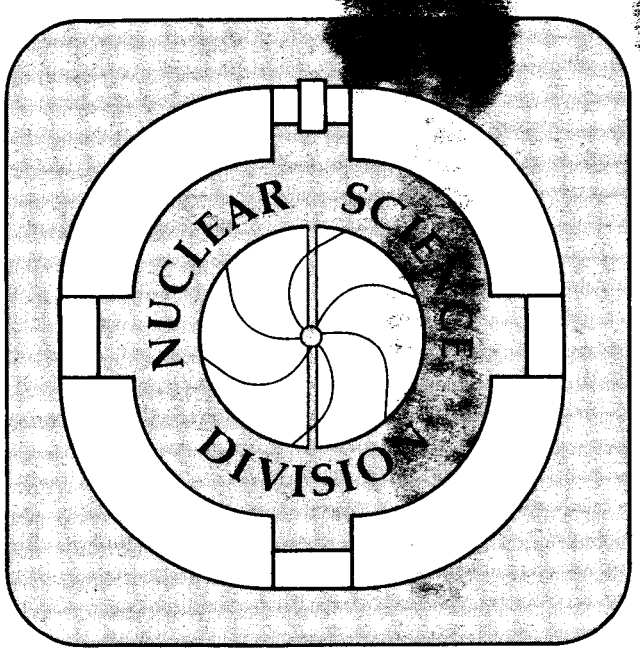

Prepared for the U.S. Department of Energy under Contract DE-AC03-76SF00098

DISCLAIMER

QUARK-GLUON PLASMA FORMATION IN THE CENTRAL RAPIDITY REGION AND FINITE SIZE EFFECTS OF COLLIDING NUCLEI

H. Sumiyoshi*

Nuclear Science Division
Lawrence Berkeley Laboratory
University of California
Berkeley, California 94720

S. Date and N. Suzuki

Department of Physics
Waseda University
Tokyo 160

O. Miyamura

Faculty of Engineering Science
Osaka University
Toyonka, Osaka 560

T. Ochiai

Department of Physics
Rikkyo University
Tokyo 171

ABSTRACT

The energy density of the central products in the ultra-relativistic heavy ion collisions are calculated. In our estimation, the special attention is paid to the space-time extension of the emission points of the secondary hadrons which are originated in the successive nucleon-nucleon interactions within the finite size of colliding nuclei. The average collision number per produced

---

*On leave of absence from Institute for Nuclear Study, University of Tokyo, Tanashi, Tokyo 188.

particle, in the final state interaction, is also calculated and is used as a criterion whether the system is thermalized or not. It turns out that the attainable energy density in the central heavy ion collision is sensitive to the space-time extension of the emission points. However, if the incident energy and the mass numbers of colliding nuclei are high and large, we can get high enough energy density for the phase transition from a hadronic state to a quark-gluon plasma state.

1. Introduction

It is now widely expected that the quark-gluon plasma (QGP) state may be created through high energy heavy ion collisions [1]. The Monte Carlo lattice gauge theory calculations [2-6] show the existence of the phase transition between the confined hadronic phase and the deconfined QGP phase. The bag model calculations [7] also give the similar prediction [7,8] for the existence of such a phase transition.

It should be inevitable, as a next step, to investigate (i) to what value the energy density of the produced system reaches through the collisions between heavy nuclei of finite sizes and (ii) whether the thermalized state can be really obtained. If the QGP state is formed, it becomes important to address (iii) what the clear signals are. From the experimental viewpoints, both in the future accelerator physics [9] and in the non-accelerator cosmic ray physics [10], not only the problem (iii) but also the systematical investigation on the incident energy per nucleon and the colliding nuclear mass number dependences of the points (i) and (ii) may become very important.

In the theoretical predictions, however, there seems to be some ambiguities in the estimation of the maximum energy densities that may be realized in both the fragmentation [11-14] and the central [15-17] rapidity regions of the ultra-relativistic nucleus-nucleus (A-A') head-on collisions. One of these uncertainties comes from the unsettled A-dependence of the rapidity density at the central rapidity region [15,18]. Another significant origin of these ambiguities seems to be in the treatment of the space-time extension of the emission

points (STEEP). Namely, particles are emitted from the extended space-time region due to the finite sizes of the colliding nuclei. This STEEP effect may be seen in every rapidity region [13,14,17]. In addition, once we take account of the STEEP effect in the calculation of the energy density, it also becomes crucial [17] how to treat the frame-independent finite hadron size, ~1 fm, conjectured by Bjorken [19].

As for the thermalization of the system produced in high energy A-A' collisions, the investigation has not been fully developed yet [8,12,17] reflecting the complexity of problems in soft QCD theory. In most of the works, the thermalization of the produced system is preassumed or only qualitative explanation to attain such a thermalized state is hopefully stated. However, under the circumstance that the inside-outside space-time structure of the hadron production holds well, the thermalization of the system is not necessarily obvious [17] and it should be investigated anyhow, quantitatively.*

In the present work in terms not of soft QCD but of hadrons, we have systematically investigated the attainable maximum energy density, ε_{max}, of the system produced in the central rapidity region through the various A-A' collisions at various incident energies. The average collision number per particle, C_π, within the system is also calculated and is used as a criterion for the thermalization of the system. On the assumption that the system is thermalized when C_π exceeds certain value, say three, we can estimate the energy density,

---

*Recently, an interesting explanation is given by Van Hove [20] although still being qualitative.

ϵ_{th}, at the thermalized stage of the system. In these calculations the STEEP effect is, of course, taken into account. The two energy densities, ϵ_{max} and ϵ_{th}, are shown in A-A' plane for various incident energies. From the results we can say that the QGP state is certainly created through the high energy heavy ion collisions if the incident energy and the mass numbers of the colliding nuclei are high and large enough. Moreover, from the study of the space-time evolution of the centrally produced system, we are able to estimate the spatial volume and the four-dimensional volume that the QGP state occupies in the A-A' collision processes.

This paper is organized as follows: In the next section, basic formula for the energy density, ϵ, is given as a function of the proper time $\hat{t}$ of the system. The STEEP effect is considered in Section 3. In Section 4, the hadron multiplicity in the system is obtained by using the multi-chain model (MCM) [21,22] for A-A' collisions [23]. Our results are given in Section 5. The final section is devoted to the discussions and conclusions.

2. Path to the QGP State Formation in A-A' Collisions

2.1. Basic Picture

We take the viewpoint that the QGP state is created through soft hadronic interactions in the A-A' collisions. In the following investigation, we will make use of the knowledge obtained from the study of the soft hadron-nucleon (h-N) and hadron-nucleus (h-A) interactions at high energies.

At first, we assume that the whole processes of an A-A' interaction are divided into three stages: (i) The nucleons in the projectile (target) nucleus successively collide with the nucleons in the target (projectile) nucleus. (ii) The secondary hadrons are produced at a proper time $\tau_0 \approx 1$ fm/c after each N-N collision. (The finite value of τ_0 corresponds to the formation zone concept [24] and leads us to what is called inside-outside space-time structure of the hadron production.) (iii) The third step is the final state interactions among the produced particles which are relevant for the thermalization of the system composed of them.

In this three step picture, it is implicit that the finally observed hadron spectra may be different from the one expected by the naive superposition of each N-N collision. Especially, once the QGP state is realized, the fluctuation of the number density in the finally observed hadron spectra may be expected [25] when the phase transition from the QGP state to the hadronic state is first order [2,6]. This reminds us of the formation of galaxies following the Big

Bang [26]. Moreover, the density fluctuation might be produced also due to the explosive process as suggested by Gyulassy et al. [27].

Further, we will pay particular attention to the facts on N-N collisions that (a) the rapidity density and the inelastic cross section, σ_{in}^{NN}, markedly increase with the incident energy above TeV region [28] and (b) the correlation length of produced particles in rapidity space is 1-2 [29].

2.2. Formulation for the Energy Density of the System

Let us consider the system composed of $N(y_1, y_2)$ hadrons that are produced within the rapidity interval between y_1 and y_2 (y_1, y_2) in an A-A' central collision. The rapidity variables are defined in the center of mass frame of the initial N-N collision. Suppose that at proper time $\hat{t}$, $N(y_1, y_2)$ hadrons occupy the space volume $V(\hat{t})$ in the comoving frame (COMF) of the system with velocity v_c:

$$v_c = \text{th } \eta = \int_{y_1}^{y_2} dy \text{ sh } y \frac{dN}{dy} \Big/ \int_{y_1}^{y_2} dy \text{ ch } y \frac{dN}{dy} \qquad (1)$$

where dN/dy is the superimposed rapidity density of all the N-N interactions in the A-A' collision. The time $\hat{t} = 0$ is defined as an instant when the hadronizations of all particles in the rapidity interval (y_1, y_2) are just completed.

The number density of the system at $\hat{t}$ is obviously given by

$$n(y_1, y_2; \hat{t}) = N(y_1, y_2)/V(\hat{t}) \quad . \tag{2}$$

Then, the energy density of the system at $\hat{t}$ becomes as

$$\epsilon(y_1, y_2; \hat{t}) = \epsilon_o \, n(y_1, y_2; \hat{t}) \tag{3}$$

where ϵ_o stands for the mean transverse mass of secondary hadrons within the system and is taken to be 0.4 GeV.

The system expands with $\hat{t}$ along the direction $\hat{z}$ of the incident nuclei. The transverse expansion of the system may be negligibly small, at least, during the early stage of the expansion [30] of the system. Then

$$V(\hat{t}) = Z^{AA}(y_1, y_2; \hat{t}) \, S_{AA'} \tag{4}$$

where $S_{AA'}$ is the overlapped area of the colliding nuclei with radii R_A and $R_{A'}$ given by $1.2 \, A^{1/3}$ fm and $Z^{AA}(y_1, y_2; \hat{t})$ is the longitudinal extension of the system. Considering the fact (b) of N-N collisions, we restrict the rapidity regions of the centrally produced system within $(y_1, y_2) = (-0.5, 0.5)$ hereafter.

3. Space-Time Extension of the Emission Points of Hadrons

3.1. Longitudinal Extension of the System in the Inside-Outside Cascade Picture

Based on the inside-outside space-time picture of hadron production, we will get the explicit formula for $Z^{AA}(y_1, y_2; \hat{t})$. For this purpose, it may be instructive to consider firstly the case that all hadrons produced in A-A' collision are emitted from one point 0 in Fig. 1. According to our assumption (ii), hadrons of rapidity y appear after τ_0 ch $(y-\eta)$ and away τ_0 sh $(y-\eta)$ from the point 0. Because we take $\hat{t} = 0$ when all the particles in the system appear as hadrons, the time difference between the point 0 and $\hat{t} = 0$ is given by τ_0 ch $(y_2 - \eta)$ (τ_0 ch $(y_1 - \eta)$) provided $|y_2 - \eta| > |y_1 - \eta|$ ($|y_2 - \eta| < |y_1 - \eta|$). In our case, $A \leq A'$ and then $|y_2 - \eta| > |y_1 - \eta|$, the system has already extended at $\hat{t} = 0$ by

$$Z_0(y_1, y_2; \hat{t} = 0) = \tau_0 \text{ ch } (y_2 - \eta) \left\{ \text{th } (y_2 - \eta) - \text{th } (y_1 - \eta) \right\}. \quad (5)$$

The system continues to expand and the longitudinal extension at $\hat{t} > 0$ becomes*

$$Z_0(y_1, y_2; \hat{t}) = Z_0(y_1, y_2; \hat{t} = 0) + \left\{ \text{th } (y_2 - \eta) - \text{th } (y_1 - \eta) \right\} \hat{t} \quad . \quad (6)$$

---

*The expression (6) corresponds to the free expansion [31] of the system and gives the upper limit of the longitudinal size of our system.

However, once we try to take the STEEP effect into account, the above expression for the longitudinal extension of the system becomes insufficient.

3.2. Geometrical Explanation of the STEEP Effect

Even if we take account of the Lorentz contraction of the colliding nuclei, they still have finite sizes. In addition, if we adopt the conjecture of Bjorken [19] that any hadrons never shrink less than 1 fm at any reference frame, the nucleons within the colliding nuclei and also nuclei themselves do not contract less than 1 fm. As a result the emission points of secondary hadrons, which stem from multiple N-N interactions within a A-A' collision, inevitably spread in $\hat{t} - \hat{z}$ plane over the diamond region OPQR as shown in Fig. 2.

The hadrons of rapidity y_1 (y_2) originated at point R(P) determine the boundary of our system on $\hat{z}$-direction. The time $\hat{t} = 0$ is taken to be the instant when the particle of rapidity y_2, which is emitted at point Q, appears within the system as a hadron.

Accordingly, the longitudinal extension of the system at $\hat{t} > 0$ is given by

$$Z^{AA}(y_1, y_2; \hat{t}) = Z_o(y_1, y_2; \hat{t} + \hat{t}_A + \hat{t}_{A'}) + L_A + L_{A'} \quad . \tag{7}$$

There are two factors that make the longitudinal distance of the system prolongate compared with the case in which emission points degenerate to the point O. One is due to the extension of the emission points to $\hat{t}$ direction;

$$\Delta Z_{\hat{t}} = \overline{AC} + \overline{BD} = Z_o(y_1, y_2; \hat{t} + \hat{t}_A + \hat{t}_{A'}) - Z_o(y_1, y_2; \hat{t}) \tag{8}$$

where

$$\hat{t}_A = \overline{OR'} = \hat{t}_Q - \hat{t}_P = \left(2R_A + S_h \text{ ch } (y_{in} + \eta)\right)\text{ch } (y_{in} - \eta)/\text{sh } (2y_{in}) \quad (9)$$

$$\hat{t}_{A'} = \overline{O'R'} = \hat{t}_Q - \hat{t}_R = \left(2R_{A'} + S_h \text{ ch } (y_{in} - \eta)\right)\text{ch } (y_{in} + \eta)/\text{sh } (2y_{in}). \quad (10)$$

As is clear from Fig. 2, the difference of the emission time between points O and Q is just $\hat{t}_A + \hat{t}_{A'}$ which leads us to (8). The other origin of the prolongation of Z^{AA} is due to the extension of the emission points to the $\hat{z}$ direction. It is nothing but the last two terms in (7) and is given by

$$\Delta Z_{\hat{z}} = L_A + L_{A'} \quad (11)$$

where

$$L_A = \overline{DF} = \overline{RR'} - \overline{TR'} = -\left\{\text{th}(-y_{in}-\eta) - \text{th}(y_1 - \eta)\right\}\hat{t}_A \quad (12)$$

and

$$L_{A'} = \overline{CE} = \overline{PP'} - \overline{SP'} = \left\{\text{th}(y_{in}-\eta) - \text{th}(y_2-\eta)\right\}\hat{t}_{A'}. \quad (13)$$

The factor S_h in (9) and (10) comes from the frame independent size [19] of nucleons. For the comparison we have also investigated the case of $S_h = 0$. In the latter case, the STEEP effect is only due to the finite sizes of the Lorentz contracted nuclei and it would disappear in the high energy limit.

Before going to the next step, one should note the following: The distance between hadrons within the system at $\hat{t} = 0$, $Z^{AA}(y_1,y_2;0)-S_h$, is about the fireball size observed by the pion interferometry [29]. Considering our path to the thermalization of the system (iii), our choice of $\Delta y = y_2 - y_1 = 1$ may be reasonable.

3.3. Average Collisioin Number per Particle in the System

During the longitudinal expansion, the hadrons in the system interact with each other and the system tends toward the thermalized state. If the interactions take place so frequently, the system will be thermalized. For simplicity, we assume that all the hadrons in the centrally produced system are pions. The mean free path of a pion in the system is given by

$$\lambda(y_1,y_2;\hat{t}) = \left\{\sigma_{in}^{\pi\pi}\, n(y_1,y_2;\hat{t})\right\}^{-1}. \tag{14}$$

As for the cross section of π–π interaction, we take the value of $\sigma_{in}^{\pi\pi}$ = 20 mb which is rather the modest value in comparison with that expected from the phase shift analysis of π–π scattering [32]. The average collision number per pion, $C_\pi(y_1, y_2;\hat{t})$, within the time interval $0 \leq \hat{t}' \leq \hat{t}$ will be obtained as follows;

$$C_\pi(y_1,y_2;\hat{t}) = \int_0^{\hat{t}} d\hat{t}'\ \bar{v}(y_1,y_2)/\lambda(y_1,y_2;\hat{t}') \tag{15}$$

$$= \frac{\sigma_{in}^{\pi\pi}\,\bar{v}(y_1,y_2)N(y_1,y_2)}{S_{AA'}\left\{th(y_2-n) - th(y_1-n)\right\}} \ln\left\{ Z^{AA}(y_1,y_2;\hat{t})/Z^{AA}(y_1,y_2;0)\right\}.$$

The mean relative velocity $\bar{v}(y_1,y_2)$ among pions in the COMF is taken to be the dispersion $\sqrt{\overline{v^2}}$, where

$$\overline{v^2} = \int_{y_1}^{y_2} dy\ th^2(y-n)\,\frac{dN}{dy} \Big/ \int_{y_1}^{y_2} dy\,\frac{dN}{dy}\,. \tag{16}$$

In our calculation, $\bar{v}(y_1,y_2) \simeq 0.27$ is almost independent of the incident energy and of the combinations of A and A'.

Before the final hadrons of rapidity y_2 appear within the system, namely at $\hat{t} < 0$, the collisions may begin to take place among pions which have already produced. In addition the collisions, that may take place in the transverse direction [15]*, are not included in (15). From these reasons, we will take rather small values of C_π, say three, as a criterion of the thermalization of the system.

It should be noticed that the role of the STEEP effect is very important in the thermalization of the system. If the emission points of hadrons shrink to one point, particles of larger rapidities always exist in the larger $\hat{z}$ regions. The resultant velocity gradient in the system is unfavorable to make it thermalize. While the STEEP effect, somewhat, randomizes the initial state of the system in the sense that particles of different rapidities occupy the same $\hat{z}$ space region.

---

*The collisions in the transverse direction may become effective for the thermalization of the system due to the STEEP effect.

4. Rapidity Density as a Superposition of N-N Collisions

4.1. Mean Collision Numbers in A-A' Collisions

The remaining point for the numerical calculation of ε and C_π is to get $N(y_1,y_2)$ in the ultra-relativistic A-A' collisions. In the high energy limit, $N(y_1, y_2)$ may be given by the product of the multiplicity $N^{NN}(y_1,y_2)$ in N-N collisions and the average total inelastic N-N collision number, $\bar{C}$, at the stage (i). Namely, at the high energy limit,

$$N(y_1,y_2) = \bar{C} \quad N^{NN}(y_1,y_2). \tag{17}$$

However, in the real case of A-A' collision the constraint of energy momentum conservation in the successive collisions becomes very important. For this reason we employ the MCM [21,22] in order to get a plausible $N(y_1,y_2)$ [23,33] even for the cases where no experimental data is available yet.

In the scheme of the MCM, A-A' collisions are considered as follows [23]: $\bar{W}_A$ ($\bar{W}_{A'}$) nucleons in the projectile (target) nucleus are wounded and each of them repeatedly interacts on average, with $\bar{\nu}_{A'}$ ($\bar{\nu}_A$) nucleons in the target (projectile) nucleus. In total, $\bar{C}$ inelastic interactions take place in an A-A' collision where

$$\bar{C} = \bar{W}_A \, \bar{\nu}_{A'} = \bar{W}_{A'} \cdot \bar{\nu}_A. \tag{18}$$

As usual, $\bar{W}$ and $\bar{\nu}$ are calculated by using Glauber formula [34] for A-A' collisions [23,35];

$$\bar{W}_A = \frac{A\int^{b_m} d^2b_I \left\{1 - \int d^2b\; t_A(b - b_I)[1-\sigma_{in}^{NN}\, t_{A'}(b_I)]^{A'}\right\}}{\int^{b_m} d^2b_I \left\{1 - [1-\sigma_{in}^{NN}\int d^2b\; t_A(b - b_I)\; t_{A'}(b_I)]^{AA'}\right\}} \tag{19}$$

$$\bar{\nu}_{A'} = \frac{A' \sigma_{in}^{NN} \int^{b_m} d^2b_I \int d^2b \; t_A(b - b_I) \; t_{A'}(b_I)}{\int^{b_m} d^2b_I \left\{ 1 - \int d^2b \; t_A(b - b_I) \; [1 - \sigma_{in}^{NN} \; t_{A'}(b_I)]^{A'} \right\}} \tag{20}$$

and

$$\bar{C} = \frac{AA' \sigma_{in}^{NN} \int^{b_m} d^2b_I \int d^2b \; t_A(b - b_I) \; t_{A'}(b_I)}{\int^{b_m} d^2b_I \left\{ 1 - [1 - \sigma_{in}^{NN} \int d^2b \; t_A(b - b_I) \; t_{A'}(b_I)]^{AA'} \right\}} \tag{21}$$

where $t_A(b)$ is the nuclear thickness defined by

$$t_A(b) = \int_{-\infty}^{\infty} dz \; \rho_A(b,z) \Big/ A \tag{22}$$

and is normalized as

$$\int d^2b \; t_A(b) = 1. \tag{23}$$

For the nuclear density, $\rho_A(b,z)$ we use the parametrization in [36]. By exchanging the role of A and A' in (19) and (20), we can get the expressions for $\bar{W}_{A'}$ and $\bar{\nu}_A$.

In (19) ~ (21), the impact parameter b_I is restricted to $0 \leq |b_I| < b_m$ (= 2 fm) to select the central A-A' collisions. Due to the restriction on b_I, even in the N-A' collision we get much larger mean collision number than the value obtained by the well-known relation

$$\bar{\nu}_{NA'} = A' \sigma_{in}^{NN} \Big/ \sigma_{in}^{NA'}. \tag{24}$$

In the A-A' collision, the above effect is prominent especially in the cases of small A and large A'. This is because most of the nucleons

in the smaller nucleus A pass through the central region of the larger nucleus A'. This inclination can be clearly seen in Table I where numerical values of $\bar{\nu}_A$, $\bar{\nu}_{A'}$, $\bar{C}$ and $S_{AA'}$ are tabulated, for various A-A' collisions at E = 1.0 TeV/N, together with $N(y_1,y_2)$ which will be obtained just after this subsection. Here

$$S_{AA'} = \int^{b_m} d^2b_I \; S_{AA'}(b_I)/\pi b_m^2 \tag{25}$$

and $S_{AA'}(b_I)$ is the overlapped area of A and A' in the transverse plane at impact parameter b_I. When we consider the case of A = A' and parameterize $\bar{C} = k_{\bar{C}} A^{\alpha_{\bar{C}}}$, $\alpha_{\bar{C}}$ becomes larger than 4/3 due to the restriction on b_I. This can be seen in Fig. 3, where $\bar{C}$, S_{AA} and $N(y_1,y_2)$ are plotted as a function of A at E = 1.0 TeV/N. The values of α and k for $\bar{C}$, S_{AA} and $N(y_1,y_2)$ are obtained by fitting the numerical results with straight lines. The numerical values of α and k are shown in Table II.

4.2. Rapidity Density and Multiplicity

From the analysis of h-A collisions it turns out that the rapidity density at the central region depends little on the way of the energy partition to the particle production in each collision [22]. Therefore, only for the simplicity of calculation we take the view of the equipartition of the energy momenta to the multiple collisions [21,22]. As a result, the desired rapidity density and the integrated multiplicity $N(y_1,y_2)$ are expressed in the following simple formula [23]:

$$\frac{dN^{ch}}{dy} = \overline{C} \int_{x_+}^{1} dx'_+ \int_{x_-}^{1} dx'_- F_{\nu_{A'}}(x'_+) F_{\nu_A}(x'_-) G\left(\frac{x_+}{x'_+}, \frac{x_-}{x'_-}\right) \tag{26}$$

and

$$N(y_1, y_2) = \frac{3}{2} \int_{y_1}^{y_2} dy \frac{dN^{ch}}{dy} . \tag{27}$$

The probability density for the equipartition distributions of the light-like momentum fraction $x'_\pm$ is given by

$$F_\nu(x'_\pm) = \begin{cases} \frac{\Gamma(\nu Q)}{\Gamma(Q)\Gamma((\nu-1)Q)} x'^{Q-1}_\pm (1 - x'_\pm)^{(\nu-1)Q-1} & (\nu \geq 2) \\ \delta(1 - x'_\pm) & (\nu = 1) \end{cases} \tag{28}$$

where the free parameter Q is taken to be unity [22] which corresponds to ν-body distribution according to their phase spaces [21].

In (26), we parameterize G as follows;

$$G(x_+/x'_+, x_-/x'_-) = \beta (1 - x_+/x'_+)^\gamma (1 - x_-/x'_-)^\gamma \tag{29}$$

and choose the parameters β and γ so as to reproduce the experimental data of N-N interaction without cut of low velocity particles. Taking account of the breaking of the scaling, we put $\beta = 2.8$ $\gamma = 3.9$ [23] and $\beta = 2.0$ $\gamma = 2.5$ [22] above and below the incident energy of 5 TeV/N, tentatively. The numerical values of $N(y_1, y_2)$ are tabulated in Table I with other quantities.* Finally it should be noted that α_N is less than $\alpha_{\overline{C}}$. This is due to the constraint of the energy momentum conservation and the effect of this constraint is clearer in lower incident energy as are shown in Fig. 3 and Table II.

---

*In the resultant rapidity density of (26) with (28), it may be slightly underestimated at both fragmentation regions and be slightly overestimated at the central rapidity region [37] in comparison with the results of the energy partition [38,39] that can reproduce well the leading particle spectra in h-A collisions.

5. The Numerical Results

5.1. Energy Density and the Average Collision Number as a Function of $\hat{t}$

The energy density of the system, composed of N(-0.5, 0.5) hadrons, are given as a function of proper time $\hat{t}$ in Figs. 4 and 5. Both of the cases, S_h = 1.0 and 0.0 fm are exhibited for F_e - F_e and U - U at E = 0.4 TeV/N (---) and 10 TeV/N (——) in Fig. 4 and for He - C (at 7 TeV/N) [40], Si - Ag (at 3.6 TeV/N) [33] and Ca - Pb (at 100 TeV/N) in Fig. 5. The values plotted along the lines are C_π's. We can judge from these figures whether the thermalized high energy density matter, the QGP state, is realized or not. We can also guess how long does such a QGP state last. One should notice that there are cases where the energy density of the system at $\hat{t}$ = 0, ϵ_{max}, is well above the critical value, say $\epsilon_c \sim$ 1 GeV/fm^3, but it becomes less than ϵ_c at the time of thermalization. In such cases, we do not consider that the QGP state is created.

5.2. Contour Plots of the Energy Density in A-A' Plane

Instead of giving full information like Figs. 4 and 5, we show the contour plots of ϵ_{max} and ϵ_{th} (ϵ at the time C_π = 3). These energy densities are depicted on A-A' half plane in Fig. 6 (S_h = 1.0 fm) and Fig. 7 (S_h = 0.0 fm) for the incident energies of E = 0.4, 1.0, 10 and 100 TeV/N. At a glance of these figures, it becomes clear how much incident energy and what kind of combinations of colliding nuclei are needed to realize the QGP state. In the contour plot of ϵ_{th}, shaded is the region where ϵ_{th} is greater than ϵ_c (=1.0 GeV/fm^3) and then the QGP state may be realized.

5.3. The Volume of the QGP State

We can get the longitudinal extension of the system at time $\hat{t}$ from (7) ~ (11). Therefore, we can estimate the spatial volume and 4-dimensional phase volume which are occupied by the QGP state within the A-A' collision processes. As a function of $\hat{t}$, Z^{AA} (-0.5, 0.5;$\hat{t}$) is given in Fig. 8 for both cases of S_h = 1.0 and 0.0 fm. Because there are no significant difference among the combinations of A and A', only the results of U - U collision at E = 0.4 and 10 TeV/N are shown. The difference of Z^{AA} between the cases of S_h = 1.0 and 0.0 fm is almost independent of $\hat{t}$ and is about 1.5 fm. We can see that this difference, 1.5 fm, is essential in the calculation of ϵ and C_π at smaller $\hat{t}$ values. See Figs. 4 and 5 and compare ϵ and C_π between the cases of S_h = 1.0 and 0.0 fm.

The maximum spatial volume, V_{QGP}^{max}, of the QGP state is obtained by

$$V_{QGP}^{max} = S_{AA'} \quad Z^{AA}(y_1,y_2;\ \hat{t}\ [\epsilon = 1,\ C_\pi > 3]). \tag{30}$$

The results are shown in Fig. 9. As a reference, the volumes of U and Fe nuclei are about 17 x 10^2 and 4 x 10^2 fm^3, respectively. Some contours in Fig. 9 disappear abruptly at halfway of the line. It means that due to the constrain of $\epsilon > \epsilon_c$, there is no region of the QGP state. V_{QGP}^{max} is at least 2 x 10^2 fm^3 and comes up to 25 x 10^2 fm^3 in the very high energy and heavy nucleus collisions. Because V_{QGP}^{max} is determined by the value of ϵ_c, it is independent of S_h only if the QGP state is realized.

In Fig. 10, 4-dimensional QGP phase volume V^4_{QGP} is shown in the unit of 10^3 x fm^4/C. V^4_{QGP} is defined by

$$V^4_{QGP} \equiv \int_{\hat{t}_{C_\pi=3}}^{\hat{t}_{\epsilon=1}} V_{QGP}(\hat{t})\, d\hat{t} \tag{31}$$

where

$$V_{QGP}(\hat{t}) = S_{AA'}\, Z^{AA}\,(y_1, y_2; \hat{t}\ [\epsilon \geq 1 \text{ and } C_\pi \geq 3]). \tag{32}$$

From V^4_{QGP} and V^{max}_{QGP}, we can guess the time interval of the QGP state lasting without breaking into the hadronic gas phase. In our calculation, the life time of the QGP state is (0.1 ~ 10) x 10^{-23} sec.

5.4. Features of E, A and S_h Dependences of ϵ and C_π

(1) E dependence: In our formulation, the incident energy dependence has been incorporated through σ^{NN}_{in}, the rapidity density $G(x_+/x'_+,\ x_-/x'_-)$ in N-N collision and Lorentz factor in (9) and (10). The increase of σ^{NN}_{in} with E brings us to the increase of $\bar{C}$ through (21) and therefore of $N(y_1, y_2)$. The rapidity density G also increase with E, although it has upper limit determined by β in (29). Moreover, the more the radii of colliding nuclei are contracted, the less the STEEP effect is. All of the energy dependences of σ^{NN}_{in}, G and Lorentz factor affect to make ϵ increase with E. C_π given by (15) also increase with E through the increase of $N(y_1, y_2)$. These inclinations agree well with our results.

(2) A-dependence: There are three competing elements which affect the values of ϵ and C_π. As A becomes larger, $\bar{C}$ increases according

to (21). This is the only element to increase ϵ and C_π with A. S_{AA}, in (4) increases with A and makes ϵ decrease with A. In addition, the STEEP effect may become remarkable with the increase of A. Therefore, contrary to the literal meaning, the STEEP effect makes the increasing rate of ϵ with A gentle. Taking all these factors into account, however, ϵ and C_π still increase with A. Namely,

$$\alpha_\epsilon \approx \alpha_N - \alpha_S - \alpha_{STEEP} > 0. \tag{33}$$

From Table II, $\alpha_N - \alpha_S > 0.57$. α_{STEEP} may be less than 0.33, then α_ϵ is positive definite.

It should be noted if we take $\alpha_N = 1.0$ [41-43] and fully take account of the STEEP effect, the increase of ϵ with A becomes much weaker than our case. In such a view, we have to rely upon the large fluctuation of the multiplicity [44] to share in the benefit of enlargening the nuclear mass numbers.

(3) S_h dependence: The inclusion of S_h in our calculation of ϵ gives rise to large STEEP effect. This is very clear in Fig. 8. However, as time elapses the effect of S_h may become obsecure due to the relation;

$$Z^{AA}(y_1,y_2;\hat{t})\Big|_{S_h=0} \Big/ Z^{AA}(y_1,y_2;\hat{t})\Big|_{S_h=1} \xrightarrow[\hat{t}\to\infty]{} 1 . \tag{34}$$

Although C_π depends on Z^{AA} only logarithmically (see (15)), the effect of including S_h is still large. This is due to the large numerical factor, which depends on A as $A^{\alpha_N-\alpha_S}$, in front of the log arithmic function.

6. Discussion and Conclusions

Our essential points in this paper are the following. One is to take account of the STEEP effect in the calculation of ϵ in A-A' collisions. The other is to impose the thermalization condition on the estimation of ϵ_{th}.

(1) Difference with and without the STEEP effect: The energy density, achieved in ultra-relativistic heavy ion collision, has been frequently estimated as follows;

$$\epsilon = \epsilon_o \frac{dN}{dy} dy/S_{AA'} \quad d\hat{z}. \tag{35}$$

In the calculation, the colliding nuclei are considered as infinitely thin pancakes. As a result, the emission points of particles in A-A' interaction shrink into one point in $\hat{z}$ direction. Therefore, we have the following one to one correspondence between y and $\hat{z}$;

$$\frac{dy}{d\hat{z}} = \frac{1}{\hat{t}} . \tag{36}$$

Then, we get

$$\epsilon = \epsilon_o \frac{dN}{dy} \Big/ S_{AA'} \cdot \hat{t}. \tag{37}$$

This relation is essentially the same as [15]. However, once the STEEP effect is taken into account, above simple formula, especially (36) does not hold. Thus our numerical results on ϵ are diluted considerably compared to the one obtained from (37) with putting $\hat{t} = 1$ fm/c.

(2) Path to the Thermalization of the System: As for the thermalization of the system, we resort to the final state interactions among hadronized particles, pions. Suppose the thermalization of

the system realizes at much earlier stage of the collision, $\hat{t} \ll 1$ fm/c, it should be asked what are the quanta which compose such a system. At least, the interactions among those quanta should be rather strong for their thermalization. However, the experimental data of high energy h-A collisions, where naive intranuclear cascade picture does not work at all, teach us that such strongly interacting quanta shortly after the collisions do not exist. Therefore, we have recognized the strongly interacting quanta that appear at proper time $\tau_0 \sim 1$ fm/C after interaction as hadron and have fully used the knowledge on hadron interaction in our calculation of ϵ and C_π.

It may be possible to replace pions in our view by the constituent quarks or valon which staisfy the quark additivity. In this case, due to the following replacement,

$$\begin{aligned} \sigma_{in}^{\pi\pi} &\to \sigma_{in}^{qq} = \frac{1}{4}\,\sigma_{in}^{\pi\pi} \\ N_\pi &\to N_q = 2N_\pi \\ \epsilon_0 &\to \frac{1}{2}\,\epsilon_0 \end{aligned} \tag{38}$$

the results of ϵ does not change but C_q, the average collision number per valon in the system, becomes half of C_π, if $\tau_0 \sim 1$ fm/C also for valons.

(3) On the freedom of the transverse direction: In our calculation the transverse expansion of the system is neglected in spite of incorporating p_T of pions through $\epsilon_0 = \sqrt{m_\pi^2 + p_T^2}$. If we assume, however, that final pions are produced via resonances or

clusters which have small transverse momenta, our idealization seems to be not so unreasonable. In this case the collisions of the resonances or clusters in the transverse direction, which may take place about the same frequencies as collisions in $\hat{z}$ direction, compensate the reduction of C_π due to the clusterization of pions. Then final results of ε_{th} may not be altered by this modification of the scenario.

(4) Miscellaneous points: (i) We have not included the particle production due to the possible cascade interactions of the secondary hadrons produced within the colliding nuclei. They may become plausible to take place especially if we adopt the finite hadron size S_h. (ii) By neglecting the finite size of produced hadrons in (5), some of hadrons that exist outside the rapidity interval (y_1,y_2) but occupy the same space volume will be effectively counted in our calculation of ε. (iii) We take a moderate value of ε_0 ($\simeq$0.4 GeV). The change in this value, for example, due to the mixture of the baryons in the central region is directly reflected to the final result of ε.

We have calculated the energy density of the central products in the ultra-relativistic A-A' collisions with taking account of the dilution factors, the STEEP effect and the finite thermalization time of the system. Even in this case, we can safely conclude that the QGP state can be obtained when the incident energy and the mass numbers of colliding nuclei are high and large.

Acknowledgement

One of the author (H.S.) is greatful to Prof. M. Gyulassy, Prof. P. V. Ruuskanen and Dr. T. Matsui for their useful discussions. He thanks Prof. J. Randrup, Dr. T. Matsui, Dr. P. Danielewicz and other members in Nuclear Science Division of Lawrence Berkeley Laboratory for their warm hospitality during his stay at LBL. He also acknowledges the financial support of Japan Society for Promotion of Science.

This work was supported by the Director, Office of Energy Research, Division of Nuclear Physics of the Office of High Energy and Nuclear Physics of the U. S. Department of Energy under Contract DE-AC03-76SF00098.

References

1. For a recent review, see (a) E. V. Shuryak, Phys. Report 61, 71 (1980); (b) M. Jacob and J. Tran Thanh Van (Eds.), Phys. Report 88 (1982); (c) M. Jacob and H. Satz (Eds.), "Quark Matter Formation and Heavy Ion Collisions", World Scientific Publishing Co., Singapore, 1982.

2. J. Engels et al., Phys. Lett. 101B, 89 (1981); Nucl. Phys. B205 [FS5], 545 (1982); J. Engels, F. Karsch and H. Satz, Phys. Lett. 113B, 398 (1982); J. Engels and F. Karsch, CERN preprint Ref. TH. 3481, Dec. 1982; T. Celik, J. Engels and H. Satz, Bielefeld preprint BI-TP 83/04.

3. L. McLerran and B. Svetitsky, Phys. Lett. 98B, 195 (1981); Phys. Rev. D24, 450 (1981).

4. J. Kuti, J. Polonyi and K. Szlachanyi, Phys. Lett. 98B, 199 (1981).

5. K. Kajantie, C. Montonen and E. Pietarinen, Z. Phys. C-Particles and Fields 9, 253 (1981); I. Montvay and E. Pietarinen, Phys. Lett. 115B, 151 (1982).

6. J. Kogut et al., Phys. Rev. Lett. 50, 393 (1983); Urbana Preprint ILL-(TH)-83-9, Apr. 198

7. S. Kagiyama et al., Prog. Theor. Phys. 62, 490 (1979); ibid 63, 956 (1980).

   M.I. Gorenstein, V.K. Petrov and G.M. Zimovjev, Phys. Lett. 106B, 327 (1981).

J. Rafelski, Proc. of the Workshop on Future Relativistic Heavy Ion Experiments, ed. R. Stock and R. Bock, GSI 81-6, Orange Report 1981, p. 282.

H. Satz, Phys. Lett. 113B, 245 (1982).

8. H. Satz, Nucl. Phys. A400, 541C (1983).
9. "The Tevalac", LBL-PUB-5081, Dec. 1982.
10. T. Saito, private communication.
11. R. Anishetty, P. Koehler and L. McLerran, Phys. Rev. D22, 2793 (1980).
12. J. Cleymans, M. Dechantsreiter and F. Halzen, Z. Physic C - Particle and Fields 17, 341 (1983).
13. K. Kajantie, R. Raito and P. V. Ruuskanen, Nucl. Phys. B222, 152 (1983); P.V. Ruuskanen, Preprint BI-TP 83/09, 1983.
14. R. Hwa, talk given at 6th High Energy Heavy Ion Study and 2nd Workshop on Anomalons held at LBL June, 1983.
15. J. D. Bjorken, Phys. Rev. D27, 140 (1983).
16. M. Gyulassy, Preprint LBL-15175 Oct. 1982; Nucl. Phys. A400, 31c (1983).
17. T. Ochiai et al., Preprint INS-Rep.-471 May 1983.
18. K. Kajantie and H. I. Miettinen, Z. Physic C - Particles and Fields 14, 357 (1982).
19. J. D. Bjorken, Proceedings of the Summer Institute on Theoretical Particle Physics in Hamburg 1975, J. G. Korner, G. Kramer and Schildknecht (Eds.), (Springer-Verlag, Berlin 1976), p. 93.
20. L. Van Hove, Preprint Ref. TH. 3592-CERN May 1983.

21. A. Capella and A. Krzwichi, Phys. Lett. 67B, 84, (1977); Phys. Rev. D18, 3357 (1978).

22. K. Kinoshita, A. Minaka and H. Sumiyoshi, Prog. Theor. Phys. 61, 165 (1979); ibid 63, 1268 (1980).

23. K. Kinoshita, A. Minaka and H. Sumiyoshi, Z. Physic C - Particles and Fields 8, 205 (1981); Proceedings of the VIth Int. Seminar on High Energy Physics Problem, Dubna, Sept. 1981, p. 334.

24. O. V. Kancheli, Pisma v ZhETF 18, 469 (1973).
N. N. Nikolaev, A. Ya. Ostapchuk and V. R. Zoller, CERN-preprint Ref. TH.2541-CERN, Sept. 1978, in which the concept of the formation zone is well summarized.

25. J. Iwai, N. Suzuki and Y. Takahashi, Prog. Theor. Phys. 55, 1537 (1976); J. Iwai et al., Nuovo Cim. 69A, 295 (1982).

26. M. Crawford and D. N. Schram, Nature 198, 538 (1982).

27. M. Gyulassy et al., Preprint LBL-16277, 1983.

28. UA5 Collab., K. Alpgard et al., Phys. lett. 107B, 310 (1981); ibid 107B, 315 (1981).

29. C. Ezell et al., Phys. Rev. Lett. 16, 873 (1977).

30. G. Baym et al., Nucl. Phys. A407, 541 (1983).

31. M. Gyulassy and T. Matsui, Preprint LBL-15947 (1983).

32. Particle Data Group, Phys. Lett. 111B, (1982).

33. JACEE Collaboration, T. H. Burnett et al., Phys. Rev. Lett. 50, 2062 (1983).

34. R. J. Glauber, Lectures in Theoretical Phys. Vol. 1 eds. W. E. Brittin and L. G. Dunham (Interscience, New York, 1959), p. 315.

35. A. Białas, M. Bleszynski and W. Czyz, Nucl. Phys. B111, 461 (1976).

36. J. W. Negele, Phys. Rev. C1, 1260 (1970).

37. H. Sumiyoshi, Phys. Lett. B131, 241 (1983).

38. K. Kinoshita, A. Minaka and H. Sumiyoshi, Prog. Theor. Phys. 63, 928 (1980).

39. A. Capella and J. Tran Thanh Van, Phys. Lett. 93B, 146 (1980); Z. Phys. C - Particles and Fields 10, 249 (1981).

40. S. Tasaka et al., Phys. Rev. D25, 1765 (1982).

41. I. Otterlund and E. Stenlund, Physica Scripta 22, 15 (1980).

42. A. Białas, Proc. of 1st Workshop on Ultra-Relativistic Nuclear Collisions, Berkeley (1979), p. 63; A. Bialas, Ref. [1(C)], p. 139.

43. S. Brodsky, J. Gunion and J. Kuhn, Phys. Rev. Lett. 39, 1129 (1977).

44. H. Ehtamo, J. Lindfors and L. McLerran, Z. Phys. C - Particles and Fields 18, 341 (1983).

Table 1. The numerical values $\bar{\nu}_A$, $\bar{\nu}_{A'}$, $\bar{C}$, N(-0.5, 0.5) and $S_{AA'}$ for various combinations of A and A' at E = 1.0 TeV/N. In the calculation, we use the value of σ_{in}^{NN} = 35 mb. Although the results are not listed here, we use the values α_{in}^{NN} 33 mb, 39 mb and 48 mb for E = 0.4, 10 and 100 TeV/N, respectively.

		C	Cu	Ag	Xe	W	U
	C	1.95					
	Cu	1.83	3.75				
ν_A	Ag	1.78	3.53	4.54			
	Xe	1.77	3.46	4.43	4.87		
	W	1.75	3.34	4.22	4.63	5.47	
	U	1.74	3.26	4.09	4.46	5.24	5.95

		C	Cu	Ag	Xe	W	U
	C	1.95					
	Cu	4.27	3.75				
ν_A	Ag	5.50	4.87	4.54			
	Xe	6.02	5.37	5.01	4.87		
	W	6.96	6.37	5.96	5.79	5.47	
	U	7.69	7.19	6.79	6.61	6.24	5.95

		C	Cu	Ag	Xe	W	U
	C	1.39					
	Cu	4.85	20.3				
C	Ag	6.48	29.2	43.7			
	Xe	7.12	33.0	50.1	57.7		
	W	8.27	39.8	62.1	72.4	92.9	
[x10]	U	9.14	45.1	71.6	77.7	110.	132.

		C	Cu	Ag	Xe	W	U
	C	3.4					
	Cu	10.3	38.9				
N	Ag	12.9	53.5	76.8			
	Xe	13.9	59.0	86.4	97.8		
	W	15.4	68.4	103.	119.	148.	
[x10]	U	16.5	75.0	115.	134.	171.	201.

		C	Cu	Ag	Xe	W	U
	C	16.5					
	Cu	23.7	59.6				
$S_{AA'}$	Ag	23.7	69.2	87.4			
	Xe	23.7	71.2	93.1	100.5		
[fm^2]	W	23.7	72.4	100.2	110.9	128.2	
	U	23.7	72.4	102.5	115.5	138.4	153.9

Table II. The numerical values of α's and k's, when we parametrize $\bar{C}$, $N(y_1,y_2)$ and S_{AA} as kA^{α}. S_{AA} is independent of the incident energy E.

E [TeV/N]	0.4	1.0	10	100
α_C	1.51	1.52	1.51	1.51
k_C	0.327	0.350	0.387	0.476
α_N	1.32	1.36	1.43	1.48
k_N	1.19	1.28	1.77	2.04
α_s	0.745	(independent of E)		
k_s [fm^2]	2.65			

Figure Captions

Fig. 1. The longitudinal expansion along with the $\hat{z}$ axis at proper time $\hat{t}$ of the system. The system is composed of particles which are within the rapidity interval (y_1, y_2) and are emitted from the point O. The emitted particles (trajectories indicated by broken lines) appear to be interactable hadrons (solid lines) when their trajectories intersect the hyperbora which corresponds to $\sqrt{\hat{t}^2 - \hat{z}^2} = \tau_0 = 1$ fm.

Fig. 2. The geometrical explanation of the STEEP effect. The emission points of hadrons are extended over the diamond region OPQR due to finite sizes of the colliding nuclei A and A'.

Fig. 3. Nuclear mass number dependences of the total collision number $\bar{C}$, hadron multiplicity $N(y_1, y_2)$ and the overlapping area S_{AA} in the central collisions of equal mass nuclei at E = 1.0 TeV/N. Those quantities are parameterized in the form of kA^{α}. The values of k and α are given by $C = 0.35\ A^{1.52}$, $N(y_1, y_2) = 1.28\ A^{1.36}$ and $S_{AA} = 2.65\ A^{0.745}$ as shown by straight lines.

Fig. 4. Energy density ϵ of the system as a function of the proper time $\hat{t}$. The numerical results of ϵ for $F_e - F_e$ ((a) and (b)) and U - U ((c) and (d)) at 0.4 TeV/N (broken curves) and 10 TeV/N (solid curves) are shown in cases of $S_h = 1.0$ fm ((a) and (c)) and $S_h = 0.0$ fm ((b) and (d)). The values written on curves are the average collision numbers per particle, C_π, by the time $\hat{t}$.

Fig. 5. The same as in Fig. 4 except combinations of A and A' and incident energies which are (a) He–C at 7 TeV/N, (b) Si–Ag at 3.6 TeV/N and (c) Ca–Pb at 100 TeV/N. The solid and broken curves correspond to the cases of S_h = 1.0 fm and 0.0 fm, respectively.

Fig. 6. Contour plots of ϵ of the system at $\hat{t} = 0$, which corresponds to ϵ_{max} and is shown in the upper triangle and at the time $C_\pi = 3$, which is ϵ_{th} and is shown in the lower triangle. S_h is taken to be 1 fm. In the shaded region, the QGP state may be realized.

Fig. 7. The same as Fig. 6 except that S_h = 0.0 fm.

Fig. 8. Z^{AA} (–0.5, 0.5; $\hat{t}$) versus $\hat{t}$ of U–U collisions at (a) 0.4 TeV/N and (b) 10 TeV/N for the cases of S_h = 1.0 fm (solid lines) and S_h = 0.0 fm (dashed lines).

Fig. 9. Contour plots for the maximum spatial volume of the QGP state, namely the spatial volume at $\epsilon = \epsilon_c$ (=1.0 GeV/fm^3). There is no region of $\epsilon \geq \epsilon_c$ at E = 0.4 TeV/N, then no contour in (a). The unit of the numerical values on the contour is 10^2 fm^3. The upper triangle is for S_h = 0.0 fm and the lower for S_h = 1.0 fm.

Fig. 10. Contour plots for the 4-dimensional phase volume of the QGP state, V^4_{QGP} which is defined in the text. The unit of the values written on the contour is 10^3 fm^4/c. The upper triangle is for S_h = 0.0 fm and the lower for S_h = 1.0 fm. By comparing Figs. 9 and 10, we can guess roughly the life time of the QGP states.

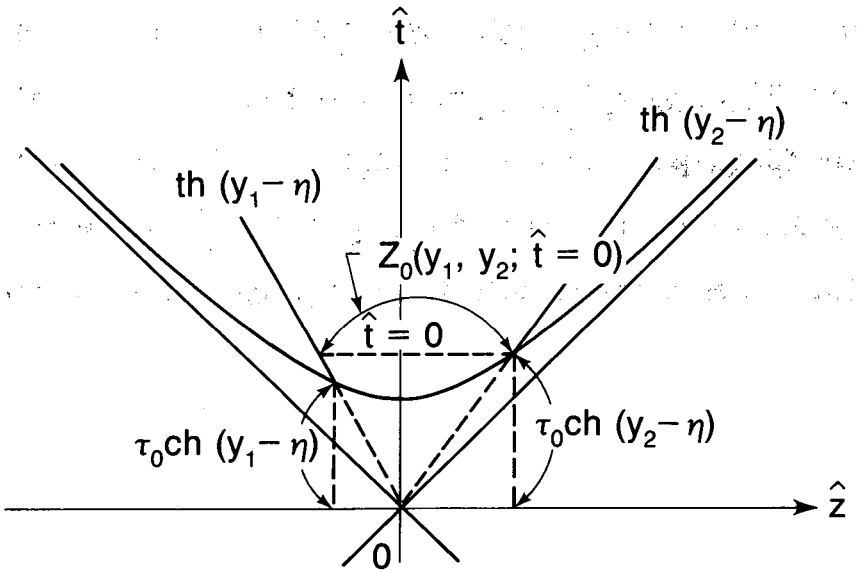

Fig. 1

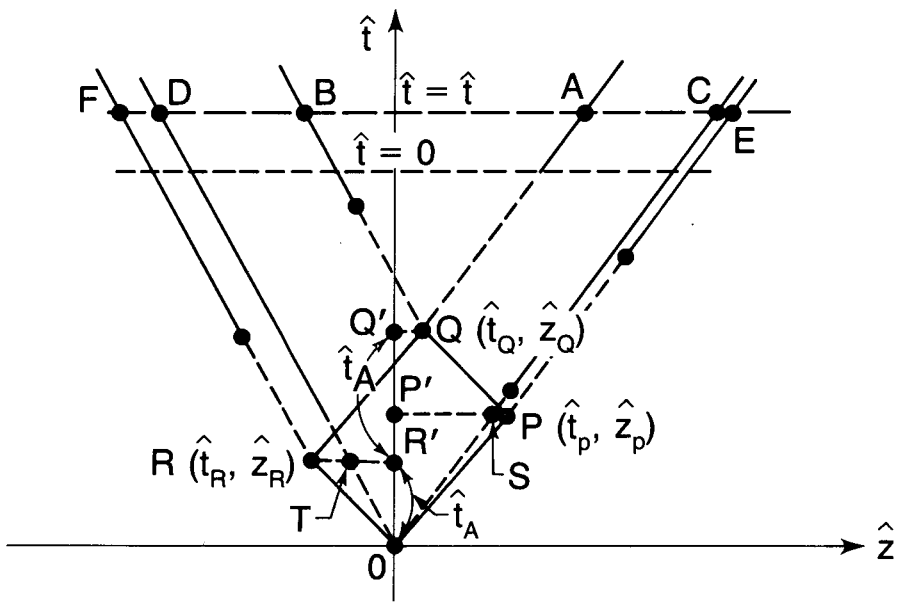

XBL 839-3260

Fig. 2

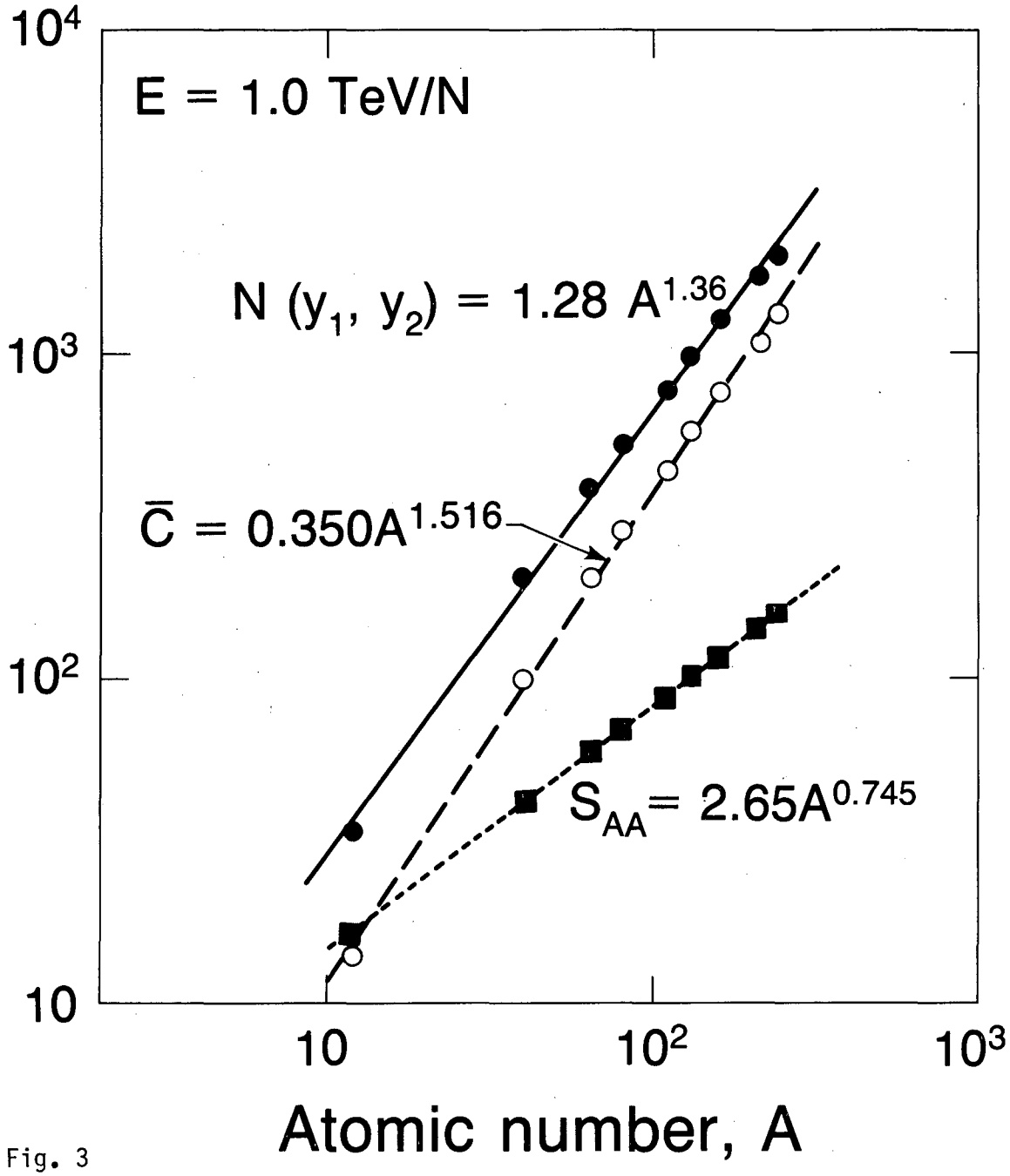

Fig. 3

XBL 839-3270

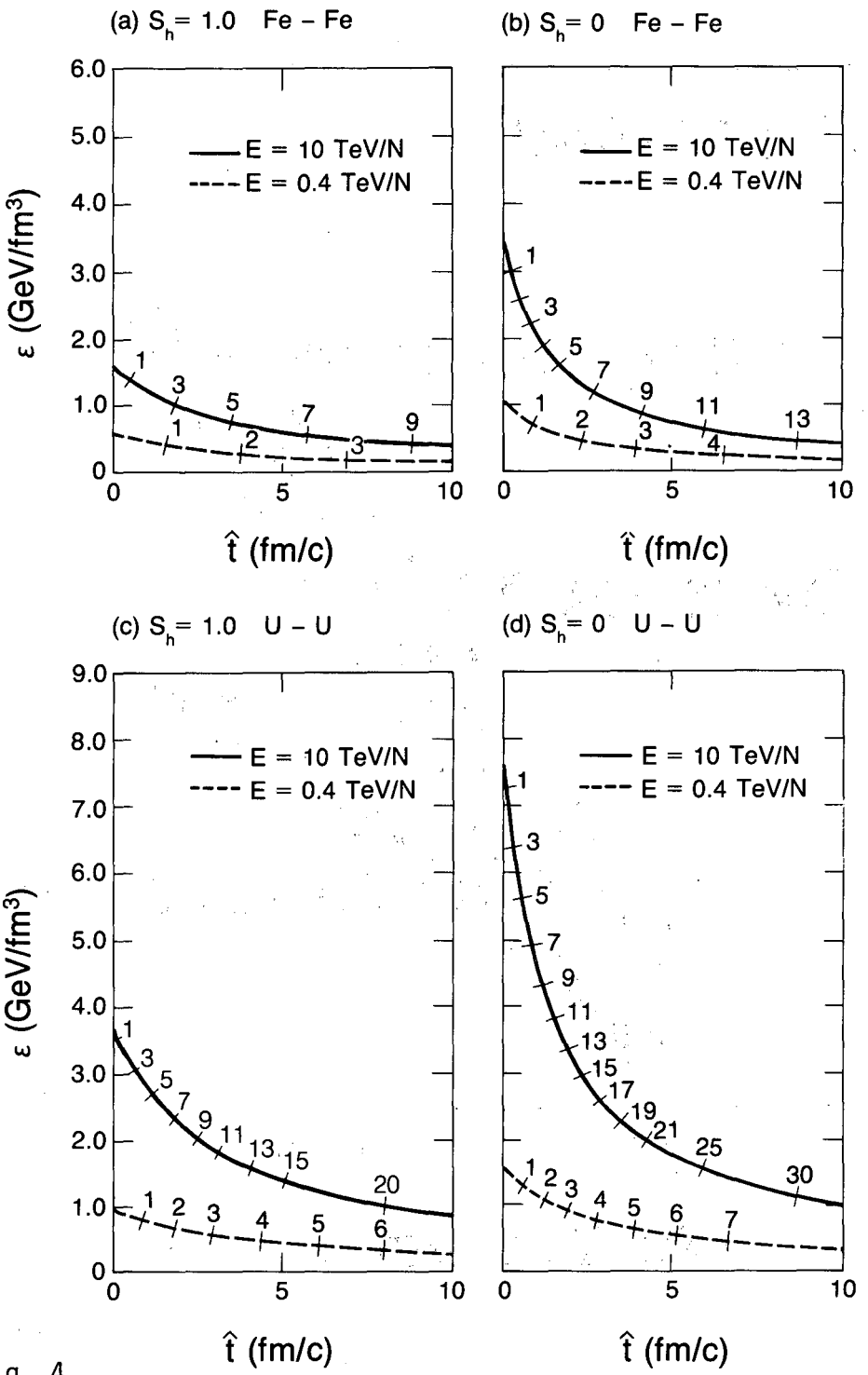

Fig. 4

XBL 839-3268

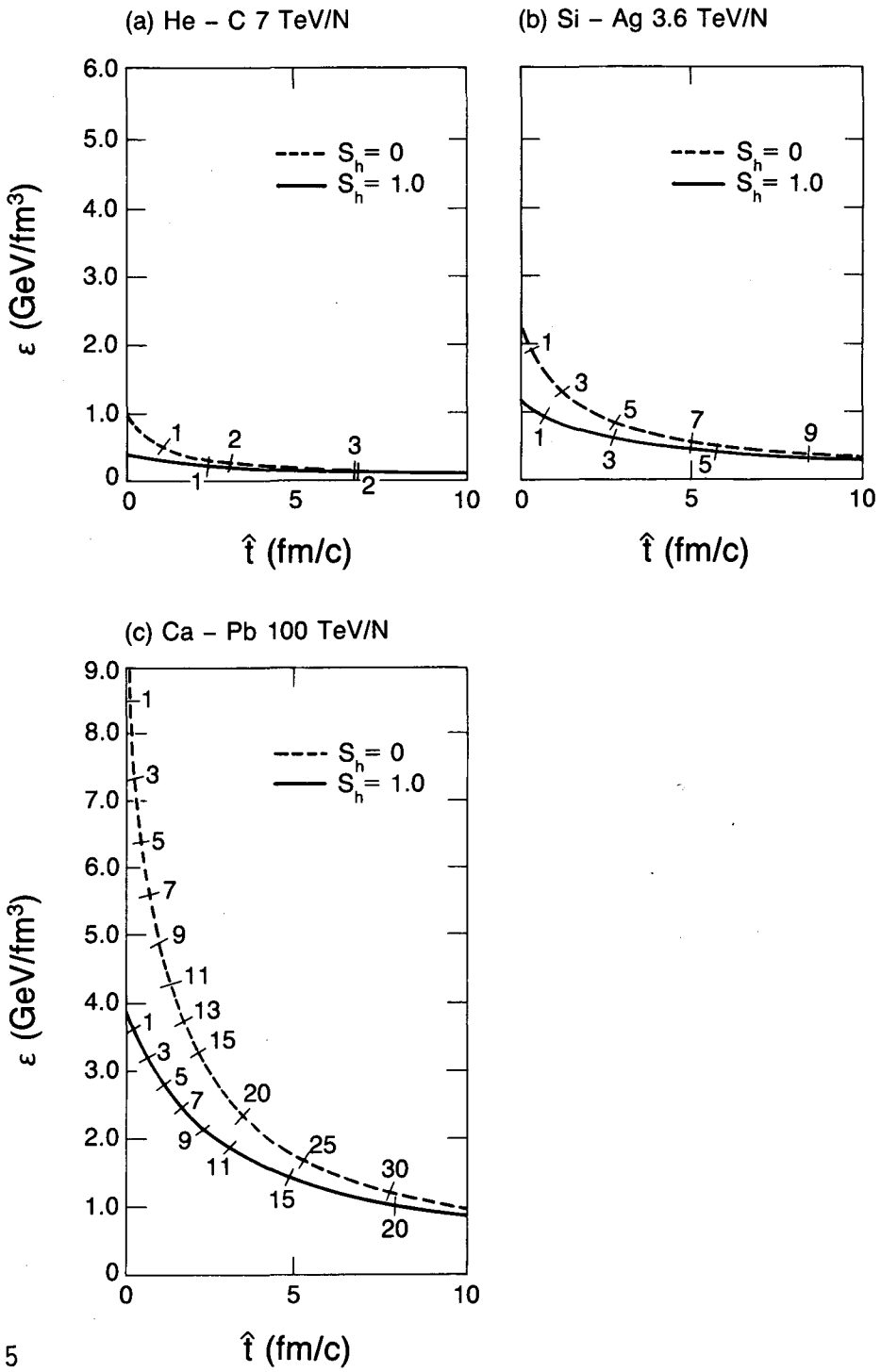

Fig. 5

XBL 839-3269

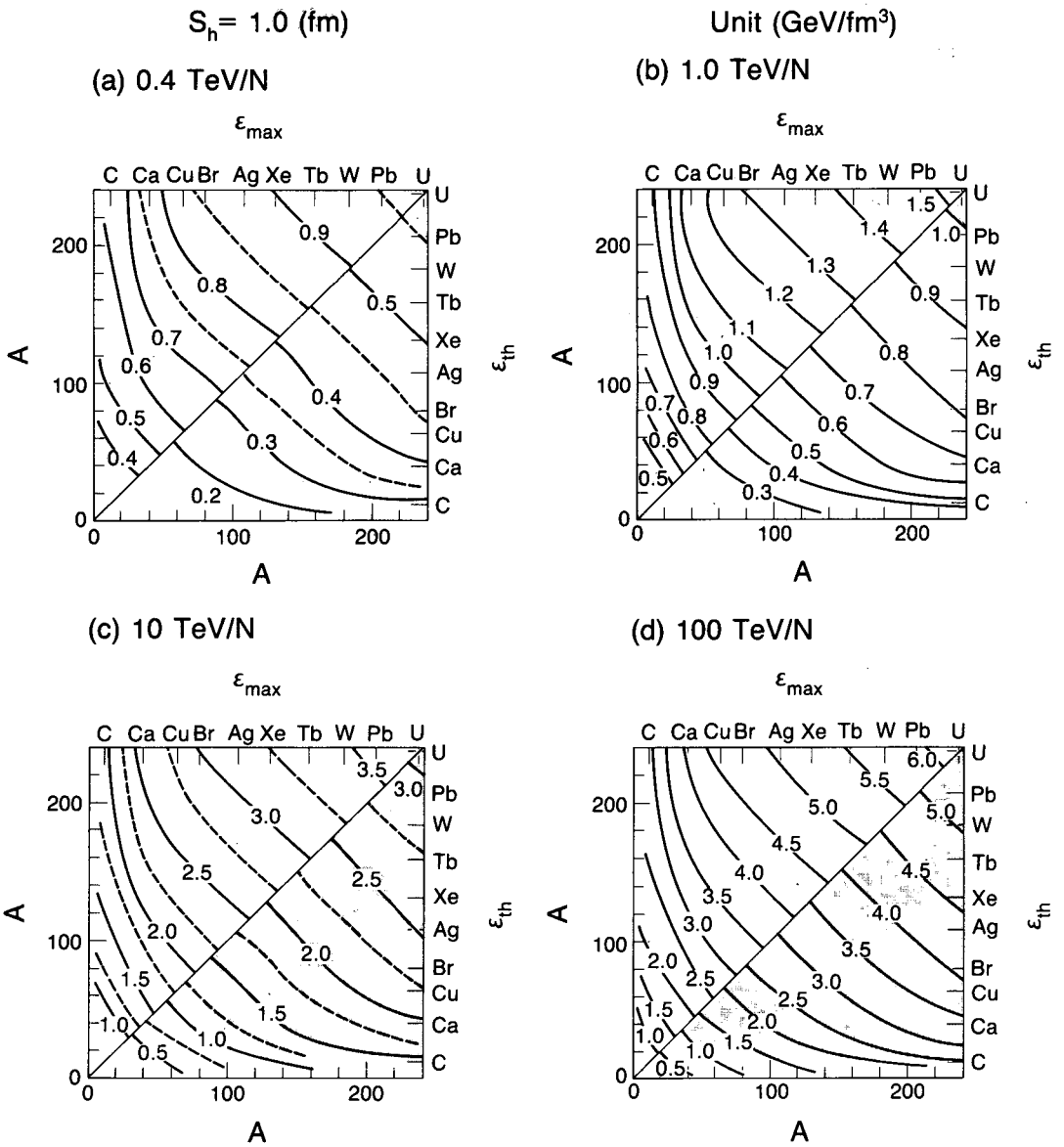
S_h= 1.0 (fm)
Unit (GeV/fm^3)
(a) 0.4 TeV/N
(b) 1.0 TeV/N
(c) 10 TeV/N
(d) 100 TeV/N
ε_{max}
ε_{th}
A
C Ca Cu Br Ag Xe Tb W Pb U
0
100
200
XBL 839-3295

Fig. 6

$S_h = 0$ (fm)

Unit (GeV/fm^3)

(a) 0.4 TeV/N

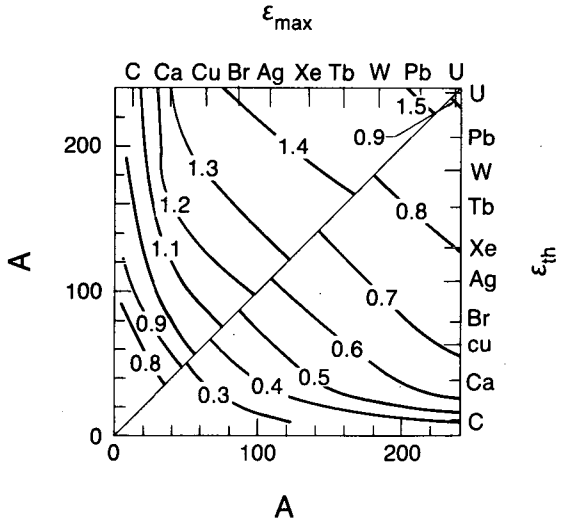

(b) 1.0 TeV/N

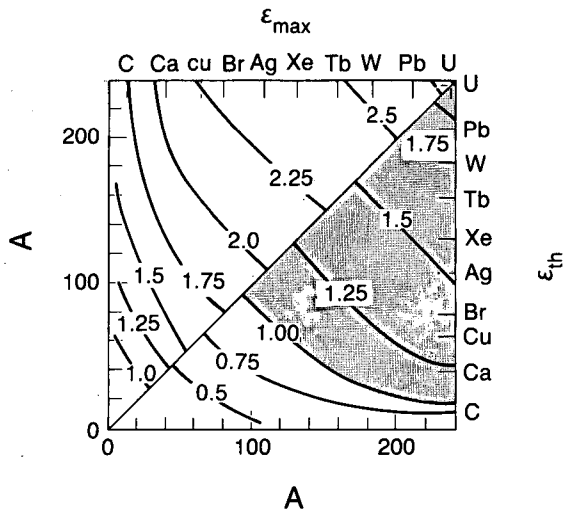

(c) 10 TeV/N

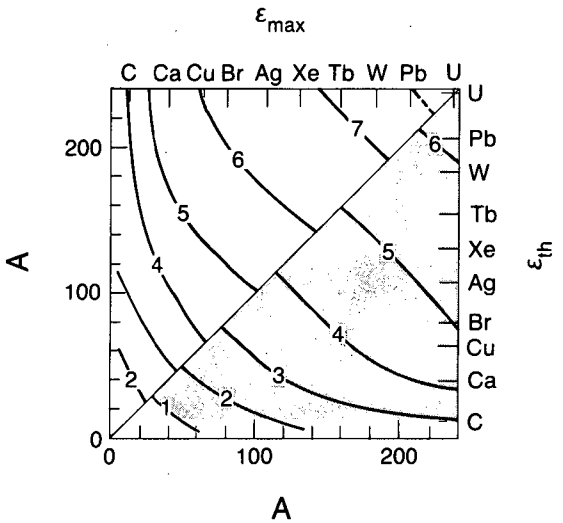

(d) 100 TeV/N

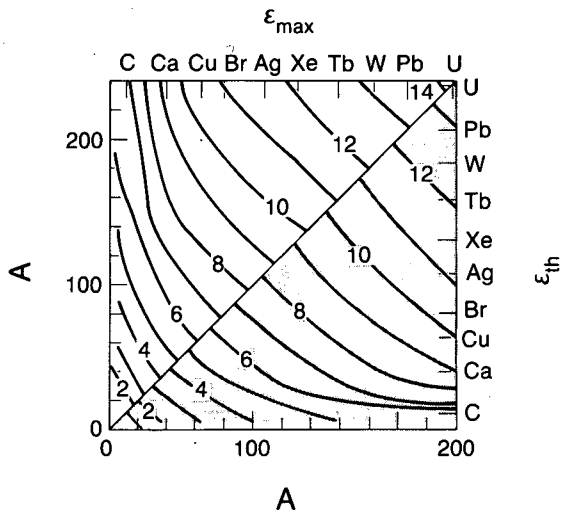

Fig. 7

XBL 839-3261

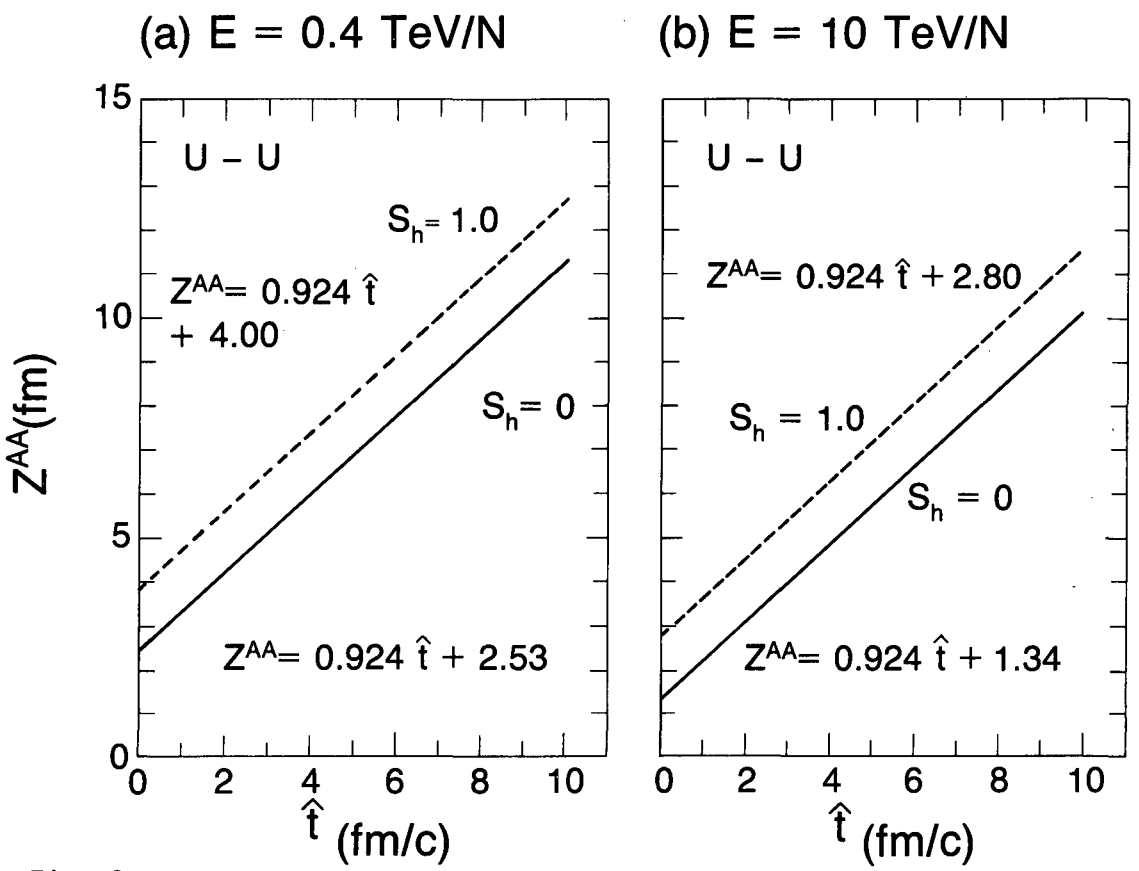

Fig. 8

XBL 839-3266

Unit ($\times 10^2 \cdot fm^3$)

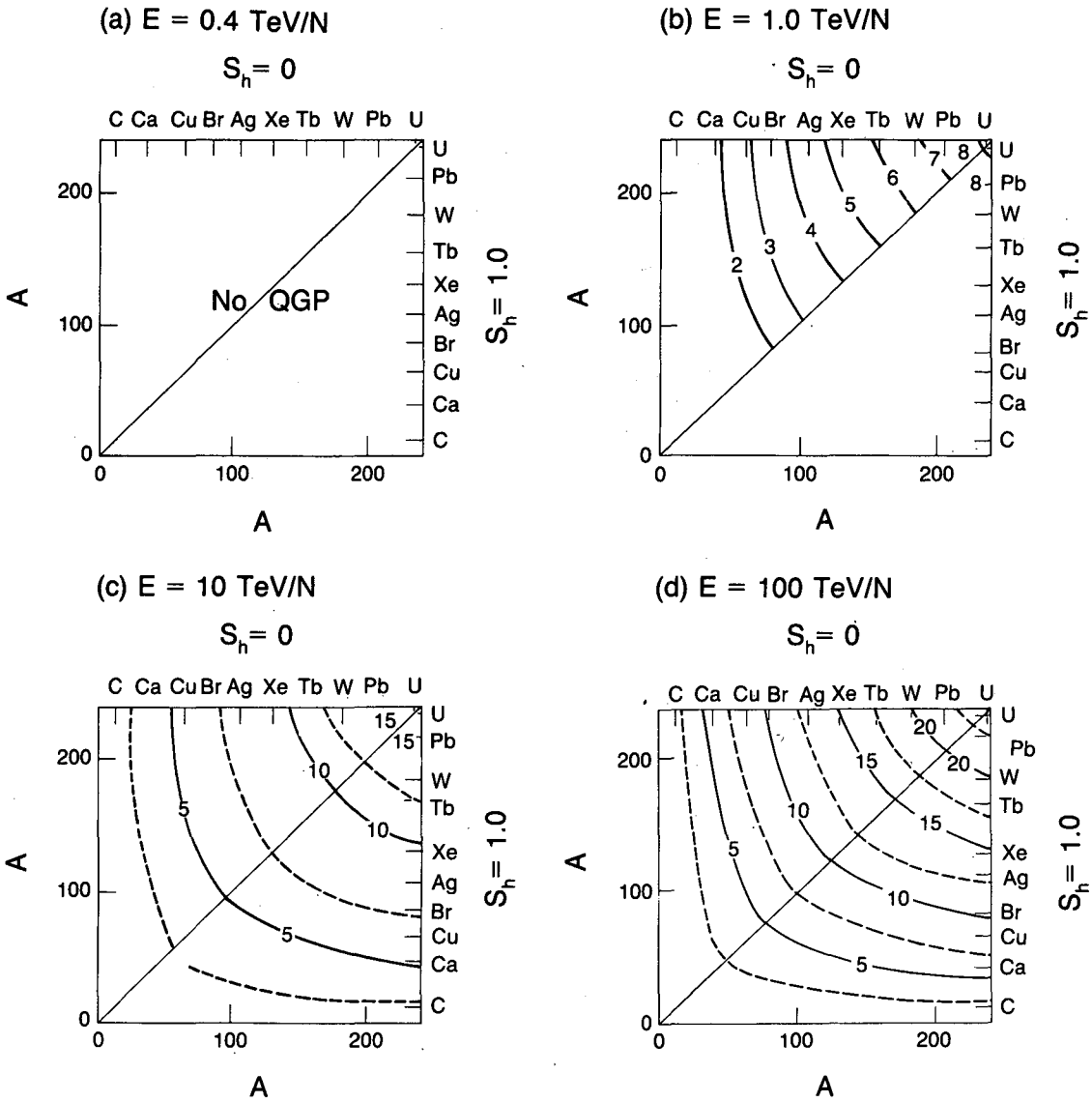

XBL 839-3267

Fig. 9

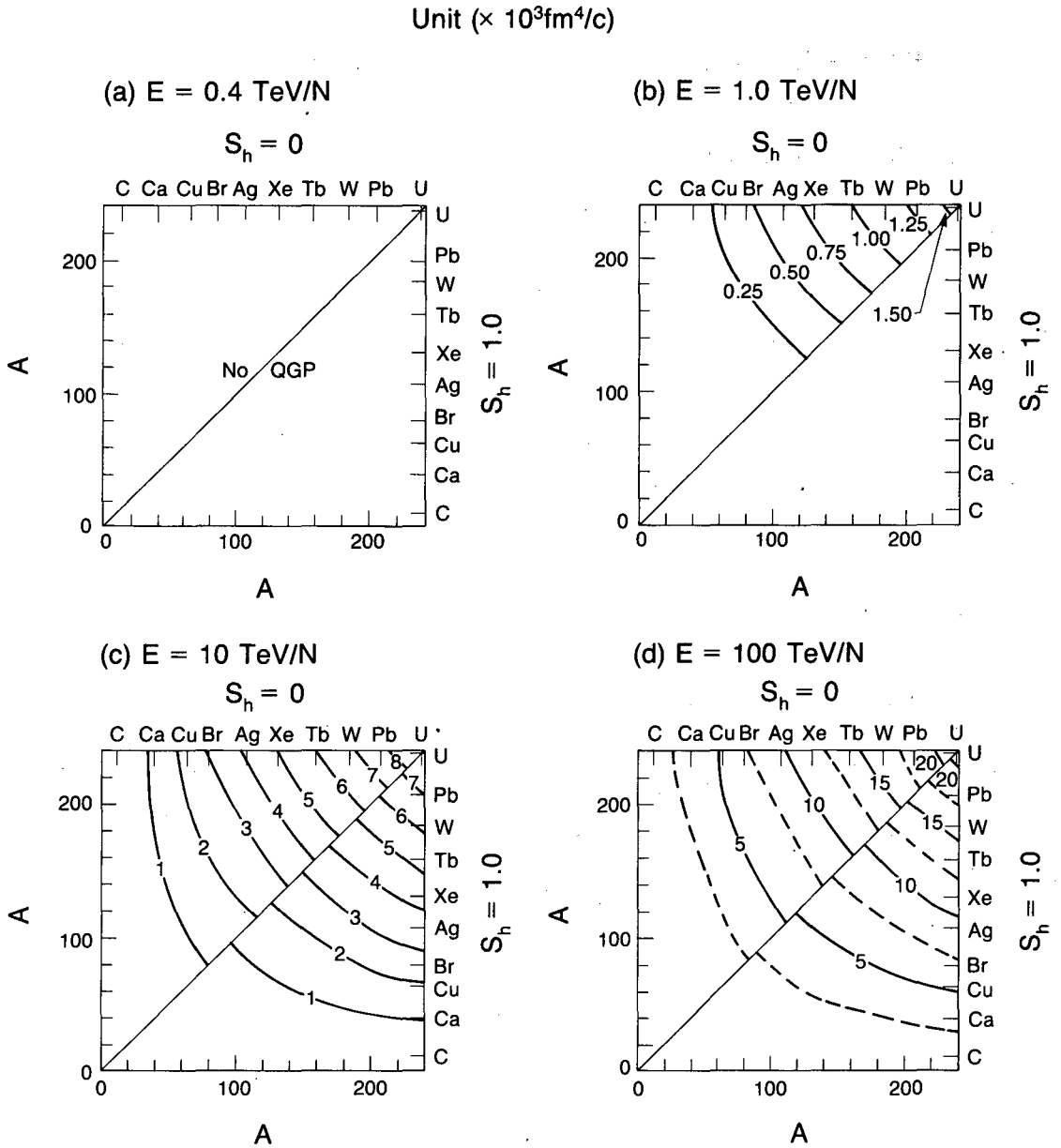

Fig. 10

XBL 839-3262

This report was done with support from the Department of Energy. Any conclusions or opinions expressed in this report represent solely those of the author(s) and not necessarily those of The Regents of the University of California, the Lawrence Berkeley Laboratory or the Department of Energy.

Reference to a company or product name does not imply approval or recommendation of the product by the University of California or the U.S. Department of Energy to the exclusion of others that may be suitable.

TECHNICAL INFORMATION DEPARTMENT
LAWRENCE BERKELEY LABORATORY
UNIVERSITY OF CALIFORNIA
BERKELEY, CALIFORNIA 94720